

Cite this: *Mater. Adv.*, 2024,  
5, 267Received 9th October 2023,  
Accepted 22nd November 2023

DOI: 10.1039/d3ma00823a

rsc.li/materials-advances

# A magnetic Fe@PANI catalyst for the selective oxidation of sulphide under mild and green conditions†

Xiaohe Wu, Ying Chen, Yiyang Zhang,  Xu Zhang\* and Lei Yu \*

The selective oxidation of sulphide to sulfoxide is an important transformation process in the industry. In this work, a novel polyaniline-supported iron catalyst (Fe@PANI) was designed and synthesised for catalyzing the reaction. It was found that the material exhibited magnetism and could be recycled by magnetic separation and reused without deactivation. The magnetic Fe@PANI-catalyzed oxidation reaction of sulphides could selectively form sulfoxides without the generation of sulfones. The inexpensive catalyst and mild and green conditions make the reaction practical for large-scale applications.

## Introduction

Sulfoxides are useful synthetic intermediates in the industry because they widely exist in a variety of medicines and pesticides, such as fipronil, lansoprazole and (*R*)-omeprazole.<sup>1</sup> Since sulphides are easily synthesized *via* nucleophilic substitution or coupling reactions, the oxidation of sulphides is considered to be a direct route to sulfoxides.<sup>2</sup> However, traditional synthesis methods encounter several issues, including the reliance on noble metals, excessive ligand consumption, the inability to recycle catalysts, the low conversion rates of catalysts, the use of chemical oxidants/additives, acidic conditions or high reaction temperatures that may be intolerable to the sensitive functional groups of the substrates.<sup>3</sup> Moreover, sulfoxides may be easily oxidized to sulfones, and controlling this side reaction is also a great challenge.<sup>4</sup> During the past decade, chemists have paid much attention to developing techniques for the selective oxidation of sulphides to sulfoxides under mild and green conditions.<sup>5</sup>

On the other hand, polyanilines (PANIs) are employed as supports to develop heterogeneous metal catalysts (M@PANIs) for a variety of reactions.<sup>6</sup> PANI-supported noble metals, such as Pd, Pt, Ag, and Au are found to be efficient catalysts in coupling reactions with very high catalyst turnover numbers (TONs).<sup>7</sup> In comparison with the inorganic supports, PANIs are versatile and their properties can be adjusted by introducing functional groups onto the aniline monomers to improve the

catalytic activities of the supported metals.<sup>8</sup> Thus, proper aniline monomers may be screened out to develop M@PANI catalysts using relatively cheap metals, such as Cu, Ni, W and Mo.<sup>9</sup> Developing iron-based catalysts is an attractive objective because Fe is the cheapest metal on earth and shows good biocompatibility with human beings and animals.<sup>10</sup> Although Fe-involved M@PANIs catalysts have already been recently reported, in most cases, Fe existed as Fe<sub>3</sub>O<sub>4</sub> to provide the magnetic property for the materials, and reports on the use of Fe@PANIs catalysts for synthesis purposes are rare.<sup>11</sup> Recently, we successfully developed a magnetic Fe@PANIs catalyst for the selective oxidation of sulphides to sulfoxides under green and mild conditions. Herein, we report our findings.

## Results and discussion

Fe@PANI materials were synthesized *via* the traditional oxidative polymerization reaction (Fig. 1). In this method, PANI monomers were initially dissolved in aqueous HCL and Fe<sub>3</sub>O<sub>4</sub> was then added as the iron source. Aqueous ammonium persulfate (APS) was then added to the system to initialize the oxidative polymerization reaction. Iron species were adsorbed onto the generated PANI fibres, which were then isolated *via* centrifugation.

Using polyaniline and *p*-fluoroaniline as monomers, we synthesized two types of Fe@PANIs and they were named Fe@PANI-H and Fe@PANI-F, respectively. Inductively coupled plasma mass spectrometry (ICP-MS) analysis indicated that the amount of Fe in Fe@PANI-H and Fe@PANI-F was 4.1% and 1.7%, respectively. The result indicated that introducing electron-withdrawing fluorine into the system could reduce

School of Chemistry and Chemical Engineering, Yangzhou University, Yangzhou, Jiangsu 225002, China. E-mail: yulei@yzu.edu.cn

† Electronic supplementary information (ESI) available: Characterization data and NMR spectra of the products. See DOI: <https://doi.org/10.1039/d3ma00823a>





Fig. 1 A diagram of the synthesis of Fe@PANI.

the coordination effect of nitrogen to metals and lead to a decrease in the Fe content.

Fe@PANI materials were synthesized *via* the traditional oxidative polymerization reaction (Fig. 1). In the method, the PANI monomers were initially dissolved in aqueous HCl, and Fe<sub>3</sub>O<sub>4</sub> was then added as the iron source. Aqueous ammonium persulfate (APS) was then added to the system to initialize the oxidative polymerization reaction. Iron species were adsorbed onto the generated PANI fibres, which were then isolated by centrifugation. Using polyaniline and *p*-fluoroaniline as monomers, we synthesized two types of Fe@PANIs and they were marked as Fe@PANI-H and Fe@PANI-F. Inductively coupled plasma mass spectrometry (ICP-MS) analysis indicated that the weight contents of Fe in Fe@PANI-H and Fe@PANI-F were 4.1% and 1.7%, respectively. The result indicated that introducing the electron-withdrawn fluorine into the system can reduce the coordination effect of nitrogen to metals and lead to a decrease in Fe content.

The materials were then employed as catalysts in the sulphide oxidation reactions (Fig. 2). Fe@PANI-F shows better catalytic activity than Fe@PANI-H, although the Fe loading is even lower in the reactions (Fig. 2a). Generally, the electron-enriched sulphides were preferable substrates, leading to higher product yields of **2a** and **2b** than the reactions of electron-deficient ones giving **2c–2e**. Introducing electron-withdrawing groups into the aliphatic chain also led to the decreased yield of **2g** (*vs.* **2f**). The reaction could be retarded by the steric hindrances of the substrates, *i.e.*, the yields of **2h** and **2i** were lower than those of **2a** and **2f**. Besides aryl, benzyl- or alkyl-substituted sulphides could also provide the related sulfoxides **2j** and **2k**, smoothly. Moreover, as a magnetic material, Fe@PANI-F could be magnetically separated after the oxidation reaction of **1a**, and it could be reused at least five times to provide **2a** in good yields (Fig. 2b). The reaction of methyl(phenyl)sulfane can be enlarged to a 10 mmol scale, giving **2a** in 91% yield. Notably, the reaction was specific for generating sulfoxides, and using excess H<sub>2</sub>O<sub>2</sub> (2.0 equiv. *vs.* 1) did not lead to any sulfone by-products, as indicated by GC-MS. Catalysed by Fe@PANI-F, thiols such as *p*-methylthiophenol could be sufficiently oxidized to produce *p*-toluenesulfonic acid only, and by using sufficient H<sub>2</sub>O<sub>2</sub> (4.0 equiv.), its yield could reach 95%.

In Fourier transform infrared (FT-IR) spectra of the materials (Fig. 3a), the peaks at 1571 and 1508 cm<sup>-1</sup> reflected the C=C stretching vibration of quinone and benzene structures. The peak strength represented the oxidation degree of PANI. The stretching vibration signals of C–N emerge at 1315 and 1240 cm<sup>-1</sup>, while the stretching vibration of C=N at 1153 cm<sup>-1</sup> is the characteristic peak of PANI. The peak at 829 cm<sup>-1</sup> is the C–H tensile vibration. The peak at 588 cm<sup>-1</sup> is the characteristic peak of Fe–O stretching vibration.<sup>12</sup> In addition, C–F stretching vibration is reflected by the signal at 707 cm<sup>-1</sup>. The introduction of the electron-withdrawing fluorine group causes the signals of stretching and bending vibrations of the chemical bonds to shift to the high-frequency direction. The high electronegativity of the fluorine group results in the increase of the strength of the peaks between 1153 to 1571 cm<sup>-1</sup>. Comparison of the FT-IR spectra demonstrates that by introducing fluorine, the electron density of the PANI chain decreased, and this may be the reason for the reduced coordination effect of nitrogen in PANI with metals leading to the decreased Fe content. However, the reduced N–Fe coordination may allow the metals to participate in the catalytic oxidation reactions more freely, resulting in the improved catalytic activity of Fe@PANI-F *vs.* Fe@PANI-H (Fig. 2).

Powder X-ray diffraction (XRD) patterns of the materials are shown in Fig. 3b. Since PANIs are polymers with low crystallinity, their diffraction peaks are low and wide, and the signals are weak. Two peaks at  $2\theta = 19.97^\circ$  and  $25.03^\circ$  are attributed to the planes (020) and (022), respectively.<sup>13</sup> The characteristic peaks of planes at (220), (311), (400), (422), (511), (440), and (511) of Fe<sub>3</sub>O<sub>4</sub> can also be observed in the XRD patterns,<sup>14</sup> indicating that iron has been successfully loaded into the material and there is no structural change of Fe<sub>3</sub>O<sub>4</sub> during the formation of the composite. The introduction of fluorine enhances the strength of the diffraction peak signal of PANI and leads to the peak shift due to the strong electronegativity of the element.

It has been reported that PANIs were mostly formed by filamentous fibres.<sup>15</sup> However, scanning electron microscopy (SEM) images of Fe@PANIs showed that introducing Fe and F may lead to changes in the morphologies and structures of the materials (Fig. 3c and d). In Fe@PANI-H, the accumulation of PANI fibres and amorphous iron particles on its surface presents a uniform particle morphology (Fig. 3c), but for Fe@PANI-F, the surface aggregations are in sheet shape with larger pores, resulting in the enhanced amount of reaction sites that can provide better contact with the reactants (Fig. 3d). Therefore, in comparison with Fe@PANI-H, the catalytic activity of Fe@PANI-F was obviously improved in sulphide oxidation reactions, regardless of the reduced Fe loading (Fig. 2).

The transmission electron microscopy (TEM) image of Fe@PANI-F shows that the outer layer of the particles of the material is covered by transparent matter, reflecting that the PANI-F covers the surface of Fe<sub>3</sub>O<sub>4</sub> (Fig. 4a). Due to the low content of iron, no crystals were detected in the electron diffraction pattern and high-resolution transmission electron microscopy (HR-TEM) image of the material (Fig. 4b and c, respectively). Energy dispersive X-ray (EDX) spectroscopy



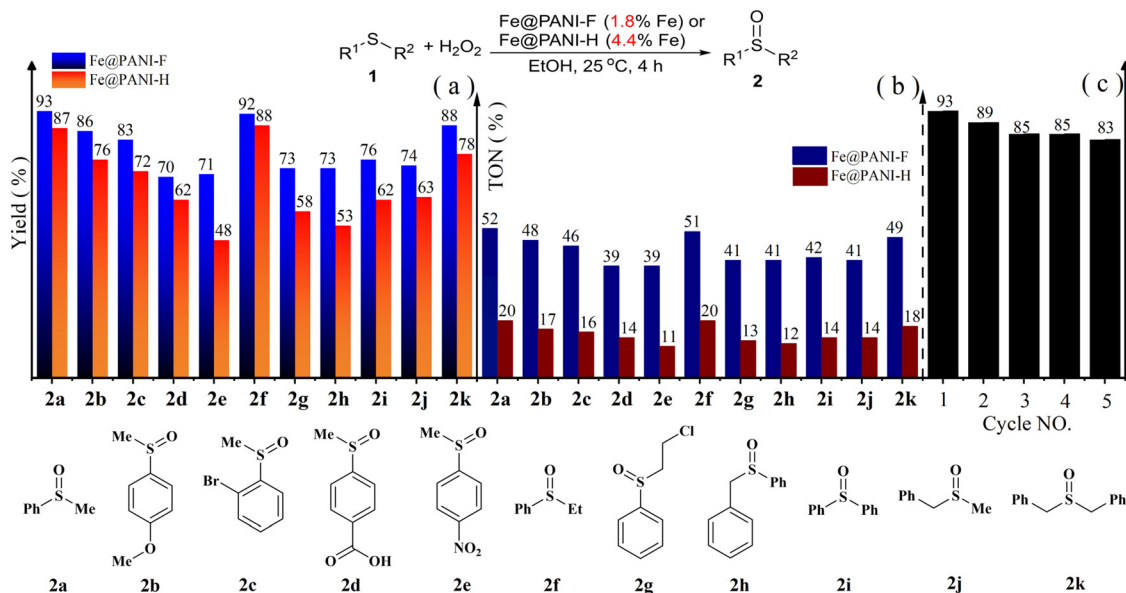


Fig. 2 The Fe@PANIs-catalyzed oxidation reactions of sulphides to sulfoxides: (a) substrate extensions, (b) TON of Fe@PANIs-catalyzed, and (c) catalyst recycling and reuse for the oxidation of **1a**.

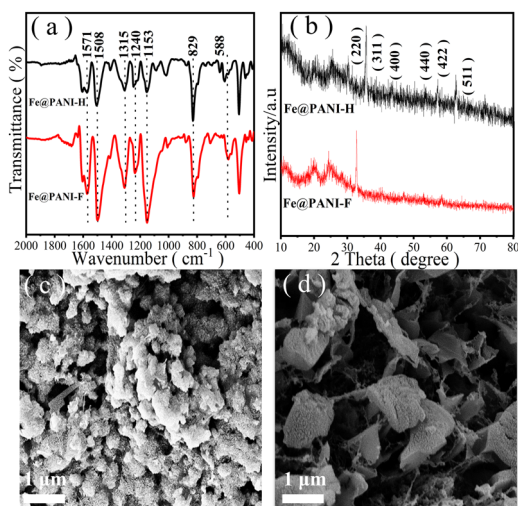


Fig. 3 The characterization of the catalysts: (a) the IR-spectra, (b) XRD patterns, (c) and (d) SEM images of Fe@PANI-H (c) and Fe@PANI-F (d).

analysis showed that Fe was involved in the material (Fig. 4d). Element mapping images demonstrated that Fe was successfully included in the skeletons of PANI-F (Fig. 4e).

In the X-ray photoelectron spectroscopy (XPS) spectra of the materials, signals at 284.6, 285.8, and 286.4 eV in the C 1s spectra are attributed to C-C/C-H, C-N/C=N, and C-O in the PANI skeleton (Fig. 5a). In N 1s spectra, the peaks at 398.7 and 401.8 eV correspond to two different chemical states of nitrogen (Fig. 5b). It is also indicated by the O<sub>1s</sub> spectra that three different states of oxygen are involved in the material, in which O<sub>c</sub> is considered to be the adsorbed oxygen, while O<sub>v</sub> is the crystal oxygen in Fe<sub>3</sub>O<sub>4</sub>, and the signal strength is determined by the oxygen vacancy concentration (Fig. 5c). In Fe<sub>2p</sub> spectra,

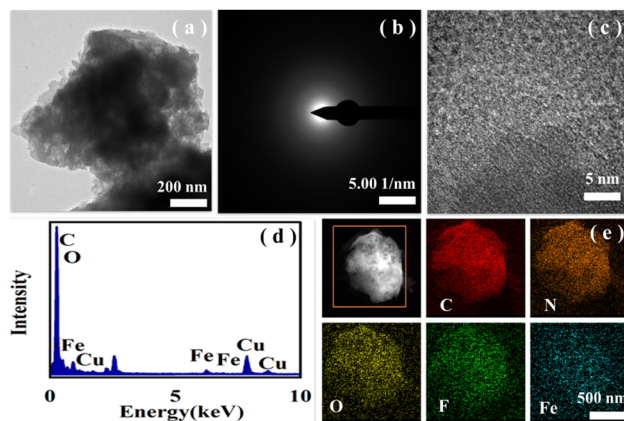


Fig. 4 The characterization of Fe@PANI-F: (a) the TEM image, (b) electron diffraction pattern, (c) HR-TEM image, (d) EDX pattern and (e) element mappings.

two signals emerged at around 711.5 and 724.7 eV, corresponding to Fe<sub>2p<sub>3/2</sub></sub> and Fe<sub>2p<sub>1/2</sub></sub>, respectively. By analysing O<sub>v</sub> and Fe<sup>δ+</sup> composition in XPS spectra, it is found that the oxygen vacancy concentration in Fe@PANI-F is higher than that in Fe@PANI-H, affording more active sites to improve the catalytic efficiency of the material in the oxidation reactions (Tables S1–S4 in ESI<sup>†</sup>).

A series of control experiments were then performed to obtain sufficient information for the mechanism study. First, using stoichiometric H<sub>2</sub>O<sub>2</sub> (1 equiv. *vs.* **1a**) resulted in decreased **2a** yield (Table 1, entries 2 *vs.* 1), and this was probably because the EtOH solvent of the reaction as a reductive chemical might have consumed a part of the oxidant. However, considering its green features as well as the cheap price, we continued to use EtOH as the solvent of the reaction.



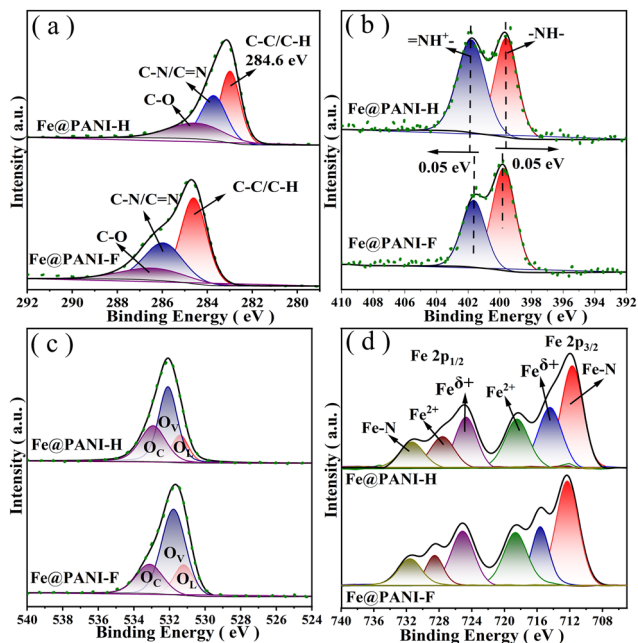


Fig. 5 The XPS spectra of the materials: (a)  $C_{1s}$ , (b)  $N_{1s}$ , (c)  $O_{1s}$  and (d)  $Fe_{2p}$ .

Further enhancing the dosage of  $H_2O_2$  could hardly enhance the product yield (Table 1, entries 3 vs. 1), but no sulfone by-product was observed by thin-layer chromatography (TLC). The result showed that the reaction condition at 25 °C could resist the over-oxidation reaction of sulfoxide to sulfone. The reaction with PANI-F as a catalyst led to **2a** in very poor yield, similar to the results of the blank reaction without a catalyst, showing that Fe was the essential catalyst for oxidation (Table 1, entries 4 and 5). Comparatively, the  $Fe_3O_4$ -catalyzed oxidation of **1a** produced **2a** in only 28% yield (Table 1, entry 6). Using soluble  $FeSO_4$  as a catalyst also led to poor **2a** yield (Table 1, entry 7). These results verified that PANI-F was an essential support that could obviously enhance the catalytic activity of Fe. Since the reaction could be restrained by 2,2,6,6-tetramethylpiperidoxyl (TEMPO), it is supposed to be a free radical reaction (Table 1, entry 8).<sup>17</sup> Salicylic acid trapping experiment further confirmed

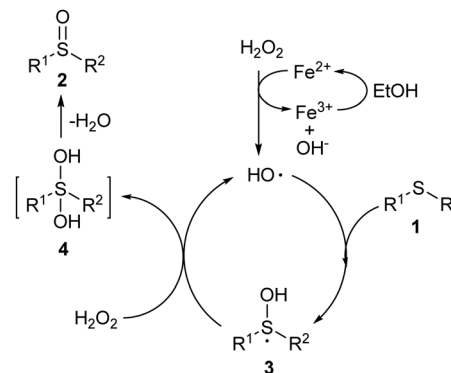
Table 1 Control experiments<sup>a</sup>

Entry	$H_2O_2/1a^b$	Catalyst, additive <sup>c</sup>	Yield <sup>d</sup> (%)
1	2.0	Fe@PANI-F (1.8)	93
2	1.0	Fe@PANI-F (1.8)	77
3	3.0	Fe@PANI-F (1.8)	92
4	2.0	PANI-F (0)	20
5	2.0	—	19
6	2.0	$Fe_3O_4$ (1.8)	28
7	2.0	$FeSO_4$ (1.8)	37
8	2.0	Fe@PANI-F (1.8), TEMPO (100)	< 5

<sup>a</sup> 0.5 mmol of **1a** was employed. <sup>b</sup> Molar ratio of the employed  $H_2O_2/1a$ .

<sup>c</sup> Percentage (%) of catalytic metal or additive vs. **1a** inside the brackets.

<sup>d</sup> Yield of **2a** on the basis of **1a**.



Scheme 1 The possible mechanism of the reaction.

that the hydroxyl radical was involved in the process (Fig. S1 in ESI<sup>†</sup>).<sup>18</sup>

Thus, on the basis of the experimental results as well as the literature reports, a plausible mechanism is proposed (Scheme 1). First, as indicated by the XPS spectra,  $Fe^{2+}$  species were involved in the material (Fig. 5d), and it could initiate the free radical chain *via* the single electron transfer (SET) reaction with  $H_2O_2$  to furnish the hydroxyl radical.<sup>19</sup>  $Fe^{2+}$  was oxidized to  $Fe^{3+}$ , which might be reduced by the organic solvent to maintain the  $Fe^{2+}$  content in the catalyst material.<sup>20</sup> The reaction of the hydroxyl radical with sulphide (**1**) led to the radical intermediate **3**, which could react with another molecule of  $H_2O_2$  to produce intermediate **4** and regenerate the hydroxyl radical to continue the radical reaction chain.<sup>21</sup> Dehydration of **4** occurred quickly to produce the final product **2**. Bearing a  $S=O$ , the electron density of sulphur in **2** significantly decreased. Thus, it could hardly react with the hydroxyl radical so the reaction could keep high selectivity at the sulphide generation step, while no sulfone by-product was produced even with an excess of the  $H_2O_2$  oxidant (Table 1, entry 3).<sup>22</sup> PANI-F is undoubtedly good support that can enhance the activity of Fe: (1) in comparison with PANI-H, the surface structure of PANI-F in the sheet shape with larger pores may enhance the number of reaction sites that can better contact with the reactants; (2) the electron-withdrawing features of fluorine group reduces the N-Fe coordination, leading to the metal participating in the catalytic oxidation reactions more freely; (3) the enhanced oxygen vacancy concentration of the catalyst after the introduction of the fluorine group may also provide more active sites for the oxidation reactions.

## Conclusions

In conclusion, we have synthesized a novel Fe@PANI-F material that can be used as an efficient catalyst for sulphide oxidation reaction to selectively produce sulfoxides. The material is magnetic and can be magnetically separated after the reaction. It can be reused at least five times giving good product yields. In comparison with references, the green and mild reaction conditions are the advantages of this method. Moreover, to the best of our knowledge, this is the first example of using



magnetic Fe@PANI materials as catalysts for synthesis purposes. Therefore, this work may inspire new ideas for the design of new catalysts in the synthesis industry.

## Experimental

### General methods

Reagents and solvents were purchased from the reagent suppliers and used directly, as received, without any special treatment. The reagents were analytically pure (AR). The melting points of the products were determined using the WRS-2A digital instrument. Fourier Transform infrared (FT-IR) spectra of the products were obtained using an Antaris II spectrometer. NMR spectra were recorded on a Bruker Avance 400 instrument using CDCl<sub>3</sub> as the solvent and Me<sub>4</sub>Si as the internal standard. Chemical shifts for <sup>1</sup>H NMR were referred to internal Me<sub>4</sub>Si (0 ppm) and J-values are shown in Hz. XPS spectra were measured on the Thermo Fisher Scientific ESCALAB 250Xi X photoelectron spectrometer. The morphologies of the catalysts were analyzed using FE-SEM on a Zeiss\_Supra55 field emission scanning electron microscope. HR-TEM images were captured on a Tecnai G2 F30 field emission transmission electron microscope. ICP-MS analysis was performed on a PerkinElmer Optima 7300 DV inductively coupled plasma spectrometer. The crystal structure of the catalyst was studied using the AXS D8 powder diffractometer at an applied current of 40 mA.

### Procedures for the preparation of Fe@PANI-F

Fe@PANI-F nanocomposites were fabricated by oxidative polymerization of 4-fluoroaniline using ammonium persulphate (APS) in an acidic medium. To a 250 mL beaker, 4.7 mL of 4-fluoroaniline and 50 mL aqueous HCl (1 mol L<sup>-1</sup>) were added. After stirring for 10 min, 200 mg of Fe<sub>3</sub>O<sub>4</sub> was added to the beaker. Then, APS solution (2.0 g APS in 40 mL 1 M HCl) was added and stirred to initiate the oxidative polymerization. The mixture was then kept standing at room temperature for 24 h, and neutralized using 1 mol L<sup>-1</sup> of aqueous NaOH. The precipitate was separated by centrifugation and washed with deionized water and EtOH 6 times. After drying at 60 °C under vacuum for 24 h, the Fe@PANI-F material was obtained.

### General procedures for the Fe@PANI-F-catalyzed selective sulfide oxidation

0.5 mmol of substrate **1**, 30 mg of Fe@PANI-F catalyst, and a piece of the magnetic bar were initially added into a 25 mL Schlenk tube. H<sub>2</sub>O<sub>2</sub> could be introduced into the system using two protocols: (1) the solution of 1 mmol of H<sub>2</sub>O<sub>2</sub> (30 wt%) in 2 mL of EtOH was injected into the system at one time; (2) the solution of 1 mmol of H<sub>2</sub>O<sub>2</sub> (30 wt%) in 2 mL of EtOH was injected into the system in four portions during the reaction processes (0.25 mmol of H<sub>2</sub>O<sub>2</sub> was added every 0.5 h). The reaction mixture was stirred at 25 °C for 4 h. After that, a magnet was placed outside the bottom of the reaction tube, while the reaction liquid was being separated. By adding fresh reactants, the recycled catalyst in the Schlenk tube can be

directly reused without any purification. The solvent in the reaction liquid was then removed by distillation with a rotary evaporator and the residue was separated by preparative TLC on silica (GF-254) with petroleum ether/EtOAc 1 : 1 to afford the related product **2**.

## Author contributions

Xiaohe Wu, Ying Chen, and Yiyang Zhang performed the experiments. Xu Zhang wrote the draft in Chinese. Lei Yu led the project, directed the students, and wrote the paper in English based on Zhang's draft.

## Conflicts of interest

The authors declare no competing financial interests.

## Notes and references

- (a) Z. Zhou, X. Wu, Z. Lin, S. Pang, S. Mishra and S. Chen, *Appl. Microbiol. Biotechnol.*, 2021, **105**, 7695; (b) X. Lin, H. Chen and Y.-N. Lin, *Ann. Palliat. Med.*, 2021, **10**, 9535; (c) T. Andersson, *Clin. Pharmacokinet.*, 1996, **31**, 9.
- (a) F. Kazemi, S. M. Naghib, Y. Zare and K. Y. Rhee, *Polym. Rev.*, 2021, **61**, 553; (b) R. Szpera, P. G. Isenegger, M. Ghosez, N. J. W. Straathof, R. Cookson, D. C. Blakemore, P. Richardson and V. Gouverneur, *Org. Lett.*, 2020, **22**, 6573; (c) F. Zhu, Z. Chen and M. A. Walczak, *J. Org. Chem.*, 2020, **85**, 11942; (d) A. C. Jones, W. I. Nicholson, H. R. Smallman and D. L. Browne, *Org. Lett.*, 2020, **22**, 7433; (e) A. Varenikov and M. Gandelman, *J. Am. Chem. Soc.*, 2019, **141**, 10994; (f) E. Voutyritsa, I. Triandafillidi and C. G. Kokotos, *Synthesis*, 2017, 917; (g) Z. Qiao and X. Jiang, *Org. Lett.*, 2016, **18**, 1550; (h) K. Kaczorowska, Z. Kolarska, K. Mitka and P. Kowalski, *Tetrahedron*, 2005, **61**, 8315.
- (a) K.-J. Liu, Z. Wang, L.-H. Lu, J.-Y. Chen, F. Zeng, Y.-W. Lin, Z. Cao, X. Yu and W.-M. He, *Green Chem.*, 2021, **23**, 496; (b) L. Tang, K. Du, B. Yu and L. He, *Chin. Chem. Lett.*, 2020, **31**, 2991; (c) J. Liu, N. Liu, H. Wang, W. Shi, J. Zhuang and X. Wang, *J. Am. Chem. Soc.*, 2020, **142**, 17557; (d) Z. Chen, C. Liu, J. Liu, J. Li, S. Xi, X. Chi, H. Xu, I.-H. Park, X. Peng, X. Li, W. Yu, X. Liu, L. Zhong, K. Leng, W. Huang, M. J. Koh and K. P. Loh, *Adv. Mater.*, 2020, **32**, 1906437; (e) K.-J. Liu, J.-H. Deng, J. Yang, S.-F. Gong, Y.-W. Lin, J.-Y. He, Z. Cao and W.-M. He, *Green Chem.*, 2020, **22**, 433; (f) R. G. Almeida, R. L. de Carvalho, M. P. Nunes, R. S. Gomes, L. F. Pedrosa, C. A. de Simone, E. Gopi, V. Geertsen, E. Gravel, E. Doris and E. N. da Silva Júnior, *Catal. Sci. Technol.*, 2019, **9**, 2742; (g) G. K. S. Prakash, A. Shakhmin, K. E. Grinton, S. Rao, T. Mathew and G. A. Olah, *Green Chem.*, 2014, **16**, 3616; (h) X. Gu, X. Li, Y. Chai, Q. Yang, P. Li and Y. Yao, *Green Chem.*, 2013, **15**, 357; (i) B. Li, A.-H. Liu, L.-N. He, Z.-Z. Yang, J. Gao and K.-H. Chen, *Green Chem.*, 2012, **14**, 130; (j) S. E. Martín and L. I. Rossi, *Tetrahedron Lett.*, 2001,



- 42, 7147; (k) A. Shaabani, Z. Hezarkhani and E. Badali, *RSC Adv.*, 2015, **5**, 61759.
- 4 (a) Q. Fan, L. Zhu, X. Li, H. Ren, G. Wu, H. Zhu and W. Sun, *Green Chem.*, 2021, **23**, 7945; (b) X. Ma, H. Hao, W. Sheng, F. Huang and X. Lang, *J. Mater. Chem. A*, 2021, **9**, 2214; (c) C. Li, N. Mizuno, K. Murata, K. Ishii, T. Suenobu, K. Yamaguchi and K. Suzuki, *Green Chem.*, 2020, **22**, 3896; (d) W. Zhao, C. Yang, J. Huang, X. Jin, Y. Deng, L. Wang, F. Su, H. Xie, P. K. Wong and L. Ye, *Green Chem.*, 2020, **22**, 4884; (e) F. Yang, X. Chu, J. Sun, Y. Zhang, Z. Li, H. Liu, L. Bai, Y. Qu and L. Jing, *Chin. Chem. Lett.*, 2020, **31**, 2784; (f) X. Lan, Q. Li, Y. Zhang, Q. Li, L. Ricardez-Sandoval and G. Bai, *Appl. Catal., B*, 2020, **277**, 119274; (g) Z. Cheng, P. Sun, A. Tang, W. Jin and C. Liu, *Org. Lett.*, 2019, **21**, 8925; (h) S. P. Das, J. J. Boruah, H. Chetry and N. S. Islam, *Tetrahedron Lett.*, 2012, **53**, 1163; (i) S. Hussain, S. K. Bharadwaj, R. Pandey and M. K. Chaudhuri, *Eur. J. Org. Chem.*, 2009, 3319.
- 5 (a) S. Liang, K. Hofman, M. Friedrich, J. Keller and G. Manolikakes, *ChemSusChem*, 2021, **14**, 4878; (b) Y. Li, S. A. Rizvi, D. Hu, D. Sun, A. Gao, Y. Zhou, J. Li and X. Jiang, *Angew. Chem., Int. Ed.*, 2019, **58**, 13499; (c) J. Zhang, T. Jiang, Y. Mai, X. Wang, J. Chen and B. Liao, *Catal. Commun.*, 2019, **127**, 10; (d) A. Bezaatpour, E. Askarizadeh, S. Akbarpour, M. Amiria and B. Babaei, *Mol. Catal.*, 2017, **436**, 199; (e) C. Su, R. Tandiana, B. Tian, A. Sengupta, W. Tang, J. Su and K. P. Loh, *ACS Catal.*, 2016, **6**, 3594; (f) S. R. Gogoi, J. J. Boruah, G. Sengupta, G. Saikia, K. Ahmed, K. K. Bania and N. S. Islam, *Catal. Sci. Technol.*, 2015, **5**, 595; (g) F. Jalilian, B. Yadollahi, M. R. Farsani, S. Tangestaninejad, H. A. Rudbari and R. Habibi, *Catal. Commun.*, 2015, **66**, 107; (h) Y. Kon, T. Yokoi, M. Yoshioka, S. Tanaka, Y. Uesaka, T. Mochizuki, K. Sato and T. Tatsumi, *Tetrahedron*, 2014, **70**, 7584; (i) J. J. Boruah, S. P. Das, S. R. Ankireddy, S. R. Gogoi and N. S. Islam, *Green Chem.*, 2013, **15**, 2944; (j) M. Jereb, *Green Chem.*, 2012, **14**, 3047; (k) B. Yu, A.-H. Liu, L.-N. He, B. Li, Z.-F. Diao and Y.-N. Li, *Green Chem.*, 2012, **14**, 957; (l) P. Zhang, Y. Wang, H. Li and M. Antonietti, *Green Chem.*, 2012, **14**, 1904; (m) A. Rostami and J. Akradi, *Tetrahedron Lett.*, 2010, **51**, 3501; (n) C. Yang, Q. Jin, H. Zhang, J. Liao, J. Zhu, B. Yu and J. Deng, *Green Chem.*, 2009, **11**, 1401; (o) W. Al-Maksoud, S. Daniele and A. B. Sorokin, *Green Chem.*, 2008, **10**, 447; (p) F. Shi, M. K. Tse, H. M. Kaiser and M. Beller, *Adv. Synth. Catal.*, 2007, **349**, 2425; (q) B. Karimi, M. Ghoreishi-Nezhad and J. H. Clark, *Org. Lett.*, 2005, **7**, 625.
- 6 (a) Z. Zeng, Y. Chen, X. Zhu and L. Yu, *Chin. Chem. Lett.*, 2023, **34**, 107728; (b) A. Yadav, H. Kumar, R. Sharma and R. Kumari, *Colloid Interface Sci.*, 2021, **40**, 100339; (c) F. Kazemi, S. M. Naghib, Y. Zare and K. Y. Rhee, *Polym. Rev.*, 2021, **61**, 553; (d) A. P. M. Udayan, O. Sadak and S. Gunasekaran, *ACS Appl. Energy Mater.*, 2020, **3**, 12368.
- 7 (a) A.-L. Wang, H. Xu, J.-X. Feng, L.-X. Ding, Y.-X. Tong and G.-R. Li, *J. Am. Chem. Soc.*, 2013, **135**, 10703; (b) Q. Dang, Y. Sun, X. Wang, W. Zhu, Y. Chen, F. Liao, H. Huang and M. Shao, *Appl. Catal., B*, 2019, **257**, 117905; (c) A. Drury, S. Chaure, M. Kröll, V. Nicolosi, N. Chaure and W. J. Blau, *Chem. Mater.*, 2007, **19**, 4252; (d) U. Bogdanović, I. Pašti, G. Ćirić-Marjanović, M. Mitrić, S. P. Ahrenkiel and V. Vodnik, *ACS Appl. Mater. Interfaces*, 2015, **7**, 28393.
- 8 Y. Liu, D. Tang, K. Cao, L. Yu, J. Han and Q. Xu, *J. Catal.*, 2018, **360**, 250.
- 9 (a) Y. Chen, L. Yu and H. Zhou, *J. Phys. Chem. C*, 2022, **126**, 17084; (b) A. Houdayer, R. Schneider, D. Billaud, J. Ghanbaja and J. Lambert, *Synth. Met.*, 2005, **151**, 165; (c) W. Li, F. Wang, Y. Shi and L. Yu, *Chin. Chem. Lett.*, 2023, **34**, 107505; (d) Y. Zhang, W. Li, Z. Hu, X. Jing and L. Yu, *Chin. Chem. Lett.*, 2024, **35**, 108938, DOI: [10.1016/j.cclet.2023.108938](https://doi.org/10.1016/j.cclet.2023.108938), in press.
- 10 (a) R. Shang, L. Ilies and E. Nakamura, *Chem. Rev.*, 2017, **117**, 9086; (b) L. Lv and Z. Li, *Top. Curr. Chem.*, 2016, **374**, 38; (c) B. D. Sherry and A. Fürstner, *Acc. Chem. Res.*, 2008, **41**, 1500; (d) C. Bolm, J. Legros, J. Le Pailh and L. Zani, *Chem. Rev.*, 2004, **104**, 6217.
- 11 (a) B. Goswami and D. Mahanta, *ACS Omega*, 2021, **6**, 17239; (b) M. N. Rantho, M. J. Madito and N. Manyala, *J. Alloys Compd.*, 2020, **819**, 152993; (c) Z. H. Dastgerdi, S. S. Meshkat, S. Hosseinzadeh and M. D. Esrafil, *J. Inorg. Organomet. Polym. Mater.*, 2019, **29**, 1160; (d) A. Fatahi, R. Malakooti and M. Shahlaei, *RSC Adv.*, 2017, **7**, 11322; (e) J. C. Apesteguy and S. E. Jacobo, *J. Mater. Sci.*, 2007, **42**, 7062.
- 12 (a) D. He, C. Zeng, C. Xu, N. Cheng, H. Li, S. Mu and M. Pan, *Langmuir*, 2011, **27**, 558; (b) O. E. Fayemi, A. S. Adekunle, B. E. Kumara Swamy and E. E. Ebenso, *J. Electroanal. Chem.*, 2018, **818**, 236.
- 13 H. C. Pant, M. K. Patra, S. C. Negi, A. Bhatia, S. R. Vadera and N. Kumar, *Bull. Mater. Sci.*, 2006, **29**, 379.
- 14 S. Erogul, S. Z. Bas, M. Ozmen and S. Yildiz, *Electrochim. Acta*, 2015, **186**, 302.
- 15 T. N. Myasoedova, T. A. Moiseeva, M. A. Kremennaya, A. Tirkeshov and G. E. Yalovega, *J. Electron. Mater.*, 2020, **49**, 4707.
- 16 T. Yamashita and P. Hayes, *Appl. Surf. Sci.*, 2008, **254**, 2441.
- 17 (a) Y. Chen, C. Chen, Y. Liu and L. Yu, *Chin. Chem. Lett.*, 2023, **34**, 108489; (b) H. Cao, P. Li, X. Jing and H. Zhou, *Chin. J. Org. Chem.*, 2022, **42**, 3890; (c) W. Zhou, X. Xiao, Y. Liu and X. Zhang, *Chin. J. Org. Chem.*, 2022, **42**, 1849.
- 18 J. Huang, R. Qian, S. Wang and H. Cao, *Chin. J. Org. Chem.*, 2021, **41**, 1639.
- 19 R. Zhu, Y. Zhu, H. Xian, L. Yan, H. Fu, G. Zhu, Y. Xi, J. Zhu and H. He, *Appl. Catal., B*, 2020, **270**, 118891.
- 20 T. de, M. Augusto, P. Chagas, D. L. Sangiorgio, T. C. de, O. MacLeod, L. C. A. Oliveira and C. S. de Castro, *J. Environ. Chem. Eng.*, 2018, **6**, 6545.
- 21 (a) A. L. Cardona, M. B. Blanco, M. A. Teruel and O. N. Ventura, *Environ. Sci.: Atmos.*, 2023, **3**, 1075; (b) Q. Ye, M. B. Goss, G. Isaacman-VanWertz, A. Zaytsev, P. Massoli, C. Lim, P. Croteau, M. Canagaratna, D. A. Knopf, F. N. Keutsch, C. L. Heald and J. H. Kroll, *ACS Earth Space Chem.*, 2021, **5**, 2013; (c) T. Berndt, J. Chen, K. H. Möller,



- N. Hyttinen, N. L. Prisle, A. Tilgner, E. H. Hoffmann, H. Herrmann and H. G. Kjaergaard, *Chem. Commun.*, 2020, **56**, 13634; (d) T. Berndt, W. Scholz, B. Mentler, L. Fischer, E. H. Hoffmann, A. Tilgner, N. Hyttinen, N. L. Prisle, A. Hansel and H. Herrmann, *J. Phys. Chem. Lett.*, 2019, **10**, 6478.
- 22 S. Liu, B. Chen, Y. Yang, Y. Yang, Q. Chen, X. Zeng and B. Xu, *Electrochem. Commun.*, 2019, **109**, 106583.

